Control of a da Vinci EndoWrist surgical instrument using a novel master controller

Sajeeva Abeywardena[1], Efi Psomopoulou, Mohammad Fattahi Sani, Antonia Tzemanaki, and Sanja Dogramadzi

Bristol Robotics Laboratory, University of the West of England, Bristol, UK
sajeeva.abeywardena@brl.ac.uk

Abstract. A novel master controller for robot-assisted minimally invasive surgery (RAMIS) is introduced and used to control a da Vinci EndoWrist instrument. The geometric model of the master mechanism and its mapping to the geometry of the EndoWrist tool are derived. Experimental results are conducted to open and close the jaws of an EndoWrist tool, and show that the developed mapping algorithm is accurate with a root mean square error of 0.7463 mm.

Keywords: Exoskeleton, robot-assisted minimally invasive surgery, geometric models, mapping

1 Introduction

Robot-assisted minimally invasive surgery (RAMIS) has gained popularity in recent decades through use of the da Vinci master-slave surgical system [1], offering improved vision, precision and patient recovery time compared to traditional MIS [2]. Typically in RAMIS, the surgeon controls the surgical instrument external from the patient's body via a master robotic controller that is not kinematically similar to the instrument tip, i.e. the da Vinci system [1] and other investigations in literature [3–6]. As such, the control of the surgical instrument is not an intuitive motion consistent with those used in open surgical techniques, i.e. grasping and cutting. Researchers have developed master controllers for uses in medical robotic interventions that are kinematically similar to the slave mechanism for more intuitive control [7, 8]. However, these are not compatible for use with the da Vinci EndoWrist instruments [9]. To offer surgeons a more anthropomorphic control interface similar to those they experience in open surgery and be able to control EndoWrist instruments, commercial data gloves or exoskeletons such as CyberGrasp [10] and Manus VR [11] could be used. However, the bulkiness and weight of such devices will hinder the performance of surgeons during RAMIS.

In this paper, a novel anthropomorphic master controller for use with daVinci EndoWrist instruments is introduced. The master controller and its geometric model are discussed in Section 2; the mapping of the geometry of the master to a da Vinci EndoWrist surgical instrument is derived in Section 3; experimental procedure and results presented in Section 4; and conclusion and future work summarised in Section 5.

2 Master Controller

The developed master controller is a 3D printed wearable exoskeleton that tracks the motion of the thumb as well as the index and middle finger. Design considerations focussed on minimising the footprint and weight of the exoskeleton. Hall-effect sensors are utilised to measure the angle of the distal interphalangeal(DIP) and proximal interphalangeal joints (PIP) of the fingers; and the interphalangeal joint (IP) of the thumb. Further, nine-degrees-of-freedom Bosch BNO-055 inertial measurement units (IMUs) are used to track the orientation of the metacarpophalangeal joints (MCP) of the thumb, index and middle fingers; as well as the carpometacarpal (CMC) joint of the thumb and the wrist. A reference IMU is placed on the dorsal side of the hand, as shown in Fig.1, for which relative orientation is calculated and thus joint angles can be derived. The exoskeleton was affixed to the wearer's hand via flexible 3D printed straps; and the CMC, wrist and reference IMUs stuck onto the hand with double-sided tape.

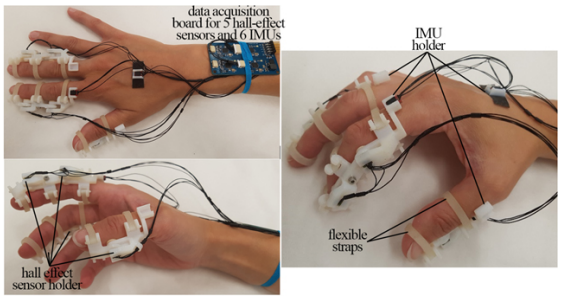

Fig. 1: The novel master wearable exoskeleton

The Direct Geometric Model (DGM) calculates the position of the thumb, index and middle fingers with respect to a global base frame. However, it is important to note that as sensors cannot be directly attached to the joints of the thumb and fingers, the DGM calculates the motion of the wearable exoskeleton which is assumed to provide a reasonable approximation to the motion of the fingers. The modified Denavit-Hartenberg (DH) notation is applied to the model of the links of the exoskeleton from which the position of the digits can be calculated.

3 Mapping Algorithm

The da Vinci EndoWrist surgical instruments consists of four-dof—roll, pitch, yaw and grasp. Roll and pitch are directly controlled by individual motors; whilst the yaw and grasp width of the instrument are dictated by the location of the

independently controlled jaws. To map between the exoskeleton and the EndoWrist instrument, the geometric models—direct and inverse (IGM)—of the instrument are required.

3.1 Direct Geometric Model

. The DGM of the jaws of the EndoWrist instrument can be derived using the modified DH parameters from which the transformation between the global base frame $\mathcal{F}_0$ and the frame of the individual jaws $\mathcal{F}_{3i}$, ${}^0\mathbf{T}_{3i}$, can be derived. To prescribe a unified motion between the jaws, a frame $\mathcal{F}_C$ was defined at the centroid of the triangle formed by vertices B_1, B_2 and B_3, defined in Fig. 2. The co-ordinates of the vertices in $\mathcal{F}_0$ can be determined from the transformation matrices previously defined. Specifically, the co-ordinates in terms of the joint-space variables $\boldsymbol{\theta} = [\theta_1, \theta_2, \theta_{31}, \theta_{32}]$ are

$$ {}^0\mathbf{b}_{1\theta} = {}^0\mathbf{T}_2\,{}^2\mathbf{l}_1 \qquad {}^0\mathbf{b}_{2\theta} = {}^0\mathbf{T}_{31}\,{}^{31}\mathbf{l}_2 \qquad {}^0\mathbf{b}_{3\theta} = {}^0\mathbf{T}_{32}\,{}^{32}\mathbf{l}_2 \tag{1} $$

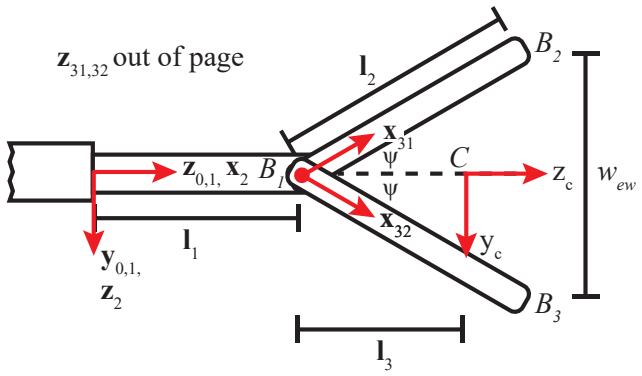

Fig. 2: Frame assignment and geometric parameters of EndoWrist instrument

As such, the origin of this frame—C—is the control point of the EndoWrist instruments. The pose of this point expressed in the base frame is ${}^0\mathbf{T}_C$, i.e.

$$ {}^0\mathbf{T}_C = \begin{bmatrix} {}^0\mathbf{Q}_C & {}^0\mathbf{p}_C \\ \mathbf{0}_{1\times 3} & 1 \end{bmatrix} \qquad {}^0\mathbf{Q}_C = [\mathbf{i}\ \mathbf{j}\ \mathbf{k}] \qquad {}^0\mathbf{p}_C = \frac{{}^0\mathbf{b}_{1\theta} + {}^0\mathbf{b}_{2\theta} + {}^0\mathbf{b}_{3\theta}}{3} \tag{2} $$

$$ \mathbf{k} = \frac{{}^0\mathbf{p}_C - {}^0\mathbf{b}_{1\theta}}{\|{}^0\mathbf{p}_C - {}^0\mathbf{b}_{1\theta}\|} \qquad \mathbf{j} = \frac{\left({}^0\mathbf{b}_{3\theta} - {}^0\mathbf{b}_{1\theta}\right) - \mathbf{k}\mathbf{k}^T\left({}^0\mathbf{b}_{3\theta} - {}^0\mathbf{b}_{1\theta}\right)}{\|\left({}^0\mathbf{b}_{3\theta} - {}^0\mathbf{b}_{1\theta}\right) - \mathbf{k}\mathbf{k}^T\left({}^0\mathbf{b}_{3\theta} - {}^0\mathbf{b}_{1\theta}\right)\|} \qquad \mathbf{i} = \mathbf{j} \times \mathbf{k} $$

3.2 Inverse Geometric Model

The IGM determines the set of joint angles $\boldsymbol{\theta}$ that will attain a specific pose ${}^0\mathbf{T}_C$. As the EndoWrist instruments have four-dof, only four-dof of ${}^0\mathbf{T}_C$ can be

directly specified. The chosen task space variables are the orientation ${}^0\mathbf{Q}_C$ and the width, w_{ew}, between the jaws of the EndoWrist instrument. The orientation is specified as the orientation of the wrist of the exoskeleton wearer, whilst the width of the jaws is correlated to the width between the tips of the index and middle finger. This width, w_{exo}, is mapped to w_{ew} as

$$w_{ew} = \frac{max_{ew} - min_{ew}}{max_{exo} - min_{exo}} w_{exo} + \frac{min_{ew} max_{exo} - min_{exo} max_{ew}}{max_{exo} - min_{exo}} \tag{3}$$

where max_j/min_j is the maximum/minimum width of the exoskeleton and EndoWrist instrument.

From Fig. 2, vertices B_1, B_2 and B_3 can be defined in $\mathcal{F}_C$ in terms of the angle ϕ, i.e.

$${}^C\mathbf{b}_{1C} = \begin{bmatrix} -\frac{2}{3} l_2 c_\phi \\ 0 \\ 0 \end{bmatrix} \qquad {}^C\mathbf{b}_{2C} = \begin{bmatrix} \frac{1}{3} l_2 c_\phi \\ l_2 s_\phi \\ 0 \end{bmatrix} \qquad {}^C\mathbf{b}_{3C} = \begin{bmatrix} \frac{1}{3} l_2 c_\phi \\ -l_2 s_\phi \\ 0 \end{bmatrix} \tag{4}$$

where $c_\phi = \cos\phi$, $s_\phi = \sin\phi$ and $\phi = \arcsin\left(\frac{w_{ew}}{2l_2}\right)$.

Equation (4) are converted into $\mathcal{F}_0$ using ${}^0\mathbf{T}_C$, whereby the position components are expressed in terms of the specified orientation ${}^0\mathbf{Q}_C$ and jaw angle ϕ, i.e.

$${}^0\mathbf{p}_C = {}^0\mathbf{Q}_2 {}^2\mathbf{l}_2 + {}^0\mathbf{Q}_C {}^C\mathbf{l}_3 \tag{5}$$

where ${}^0\mathbf{Q}_2$ only takes into account roll and pitch of ${}^0\mathbf{Q}_C$, ${}^2\mathbf{l}_2$ is the vector from the origin of $\mathcal{F}_0$ to vertex B_1 and ${}^C\mathbf{l}_3$ is the vector from the vertex B_1 to the origin of $\mathcal{F}_C$.

As the vertices B_1, B_2 and B_3 are specified in terms of the joint angles and task space variables through Eq. (1) and Eq. (4), the following holds

$${}^0\mathbf{b}_{iC} = {}^0\mathbf{b}_{i\theta} \tag{6}$$

for $i = 1, 2, 3$. As such, there are 9 equations in terms of 4 unknowns—the joint space variables. Thus, solving these equations provides the solution to the IGM.

4 Experimental Setup

The master controller was used to control a 8 mm EndoWrist ProGrasp Forceps, as shown in Fig. 3, which was actuated by four Maxon brushed DC motors. The motors interfaced with a custom built motherboard that consisted of ePos2 control modules. A master-slave Arduino setup was utilised for the master controller. The sensors interfaced with a custom built motherboard that consisted of four Arduino Uno chips that communicated via SPI with a master Arduino Uno board. This board in turn communicated with a PC via serial. The exoskeleton and instrument were interfaced in Linux and communicated via ROS.

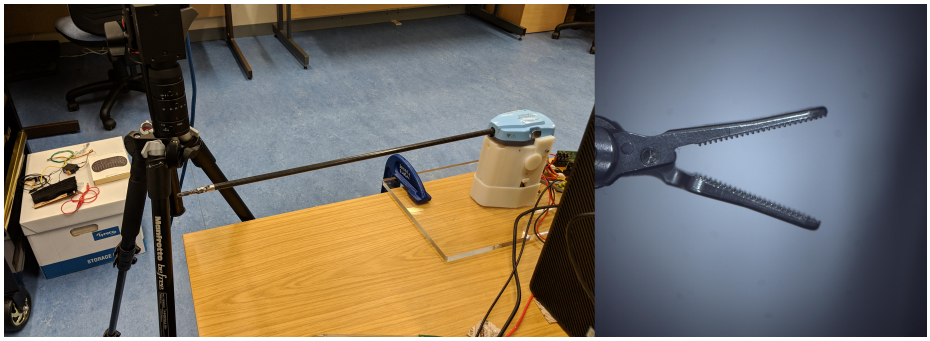

Fig. 3: ProGrasp Forceps (left) and example capture of instrument tip (right)

4.1 Results

Investigation into the accuracy of the mapping algorithm was conducted, specifically focussing on grasp width. A camera was used to track the motion of the jaws of the ProGrasp forceps in a two-dimensional plane, with an example capture provided in Fig 3. The results from an experiment in which the jaws were continuously opened and closed are shown in Fig. 4. This experiment yielded a root mean square error of 0.7463 mm. The EndoWrist instruments are cable driven with base-located motors, i.e. motors are not directly attached to the joints of the instrument-tip. Thus, cable tension and losses such as friction and hysteresis will affect the motion transmitted to the tool tip, i.e. why desired and measured width differ. As evident in Fig. 4, this is most apparent when closing the jaws. Nevertheless, the magnitude of error shows the mapping algorithm to be relatively accurate for the grasping dof.

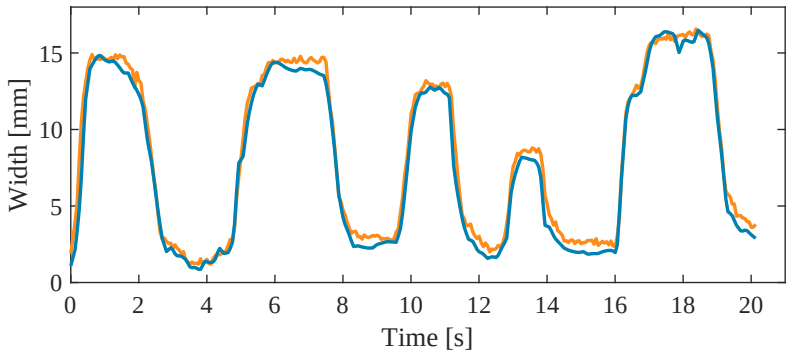

Fig. 4: Experimental results: command width (blue), measured width (orange)

5 Conclusion and Future Work

A novel master controller for RAMIS was introduced. The geometric model of the master mechanism was summarised and its mapping to the motion of the EndoWrist tool derived. Experimental results showed that the developed mapping algorithm is accurate in the grasping dof, which provides promise for the use of the novel master controller in RAMIS. Future work will integrate the master controller with a Haption Virtuose6D desktop device to provide control of the roll of the EndoWrist instrument, investigate the accuracy of the other dof, as well as assess the efficacy of this controller compared to the standard da Vinci master controller. Further, the use of the wearable exoskeleton to control a novel anthropomorphic surgical instrument will be investigated.

Acknowledgements

This work was supported by the European Union's Horizon 2020 research and innovation programme under grant agreement No 732515.

References

1. https://www.intuitive.com/
2. Lanfranco, A.R., Castellanos, A., Desai, J., Meyers, W.: Robotic surgery: A current perspective. Annals of Surgery **239**(1), 14–21 (2004)
3. Arata, J., Mitsuishi, M., Warisawa, S., Tanaka, K., Yoshizawa, T., Hashizume, M.: Development of a dexterous minimally-invasive surgical system with augmented force feedback capability. In: 2005 IEEE/RSJ International Conference on Intelligent Robots and Systems, pp. 3207–3212 (2005)
4. Thielmann, S., Seibold, U., Haslinger, R., Passig, G., Bahls, T., Jrg, S., Nickl, M., Nothhelfer, A., Hagn, U., Hirzinger, G.: Mica - a new generation of versatile instruments in robotic surgery. In: 2010 IEEE/RSJ International Conference on Intelligent Robots and Systems, pp. 871–878 (2010)
5. Hannaford, B., Rosen, J., Friedman, D.W., King, H., Roan, P., Cheng, L., Glozman, D., Ma, J., Kosari, S.N., White, L.: Raven-ii: An open platform for surgical robotics research. IEEE Transactions on Biomedical Engineering **60**(4), 954–959 (2013)
6. Talasaz, A., Trejos, A.L., Patel, R.V.: The role of direct and visual force feedback in suturing using a 7-dof dual-arm teleoperated system. IEEE Transactions on Haptics **10**(2), 276–287 (2017)
7. Ikuta, K., Hasegawa, T., Daifu, S.: Hyper redundant miniature manipulator "hyper finger" for remote minimally invasive surgery in deep area. In: 2003 IEEE International Conference on Robotics and Automation (Cat. No.03CH37422), vol. 1, pp. 1098–1102 vol.1 (2003)
8. Zhang, L., Zhou, N., Wang, S.: Direct manipulation of tool-like masters for controlling a masterslave surgical robotic system. The International Journal of Medical Robotics and Computer Assisted Surgery **10**(4), 427–437 (2014)
9. https://www.intuitive.com/en-us/products-and-services/da-vinci/instruments
10. http://www.cyberglovesystems.com/cybergrasp
11. https://manus-vr.com